DALTON

Kinetic and thermodynamic studies of intramolecular rearrangement and cleavage of the heterobinuclear aqua ion, $[(H_2O)_4Rh(\mu\text{-}OH)_2Cr(OH_2)_4]^{4+}$

Stephen J. Crimp and Leone Spiccia *

Department of Chemistry, Monash University, Clayton, Victoria, 3168, Australia

The doubly bridged (d.b.) heterobinuclear aqua ion $[(H_2O)_4Rh(\mu\text{-}OH)_2Cr(OH_2)_4]^{4+}$ was converted into a singly bridged (s.b.) form $[(H_2O)_5Rh(\mu\text{-}OH)Cr(OH_2)_5]^{5+}$ in strongly acidic solution. Pure solutions of the latter were obtained using low-temperature ion-exchange chromatography. Its cleavage is much slower than interconversion between the d.b. and s.b. forms. In the range pH 0–1 both forms exist in measurable concentrations, allowing equilibrium measurements to be made. The variation in the relative concentrations of the two forms with $[H^+]$ has been interpreted in terms of two equilibria: deprotonation/protonation of the s.b. form and equilibration between monodeprotonated (s.b. − H) and d.b. forms. The high acidity of the s.b. form is due to the high charge and hydrogen-bond stabilisation of s.b. − H. The pH dependence of k_{obs} for the interconversion between the s.b. and d.b. forms of the aqua ion has been interpreted in terms of five reaction pathways: ring closure within s.b., s.b. − H and s.b. − 2H, and ring opening within protonated d.b. and d.b. Only small enhancements in ring-closure rates were observed on deprotonation of the s.b. form when compared with the related chromium(III) systems. Acid cleavage of $[(H_2O)_4Rh(\mu\text{-}OH)_2Cr(OH_2)_4]^{4+}$ to Cr^{3+} and Rh^{3+} was found to proceed *via* the s.b. and s.b. − H forms, the acid dependence of the rate constant being due to equilibration between the s.b. and d.b. forms. Cleavage of the s.b. form is at least 100 times slower than conversion of the d.b. into the s.b. form. The similarity in the rates and activation parameters, for both the interconversion and cleavage reactions, to those reported previously for the corresponding chromium(III) dimer indicates that the reactions of $[(H_2O)_4Rh(\mu\text{-}OH)_2Cr(OH_2)_4]^{4+}$ are Cr^{III} centred substitution processes.

We have recently reported the synthesis of the first heteronuclear aqua ion containing rhodium(III) and chromium(III) centres linked exclusively by hydroxide bridging groups,[1] $[(H_2O)_4Rh(\mu\text{-}OH)_2Cr(OH_2)_4]^{4+}$. It can be obtained in good yield by treating Cr^{3+} with Rh^{3+} in alkaline solution and the structure of the mesitylene-2-sulfonate salt has been determined.[1] An acid-dependent equilibrium was found to exist between this doubly bridged (d.b.) form and the singly bridged (s.b.) form, $[(H_2O)_5Rh(\mu\text{-}OH)Cr(OH_2)_5]^{5+}$. We report here kinetic and thermodynamic investigations of the intramolecular rearrangement between the two forms of this aqua ion and the kinetics of cleavage to Cr^{3+} and Rh^{3+}. This is the first study of the hydrolytic processes involved in the cleavage and rearrangement of a heterobinuclear aqua ion. The chromium(III) dimer $[(H_2O)_4Cr(\mu\text{-}OH)_2Cr(OH_2)_4]^{4+}$ is the only other binuclear aqua ion to have been studied extensively.[2–5]

Experimental

Materials

Solutions of $[(H_2O)_4Rh(\mu\text{-}OH)_2Cr(OH_2)_4]^{4+}$ and the corresponding 'active' hydroxide $[RhCr(\mu\text{-}OH)_2(OH)_4(OH_2)_4]$ were prepared and purified as described previously for the rhodium(III) dimer.[6] The term 'active' refers to the fact that this hydroxide dissolves rapidly in acid regenerating the heterobinuclear aqua ion. All materials were of LR grade or better and were used as received, although for quantitative measurement AR reagents were used. Cation-exchange chromatography was carried out on Sephadex SP C25 resin (Pharmacia). All solutions were prepared with distilled water and filtered through Millipore filters (GSWP, 0.22 μm) before use. Standard solutions of $LiClO_4$ and $NaClO_4$ were made by neutralising standard solutions of LiOH and NaOH with $HClO_4$.

Supplementary data available (No. SUP 57117, 7 pp.): observed rate constants for acid cleavage and rearrangement. See Instructions for Authors, *J. Chem. Soc., Dalton Trans.*, 1996, Issue 1.

Instruments and methods

A Cary 3 spectrophotometer, fitted with a Cary temperature controller (± 0.1 K) and a multiple-cell compartment, was used to record UV/VIS spectra and to carry out kinetic experiments. Calibrated temperature probes were used accurately to measure the temperatures of the reaction mixtures directly in the cell compartment. The method for measuring pH has been described previously.[2]

Chromium(III) was found to interfere with the analysis of rhodium by the $SnCl_2$–HCl method.[7] Rhodium analyses on solutions containing both Rh^{III} and Cr^{III} were carried out using the hypochlorite method developed by Ayres and Young.[8]

Synthesis of $[(H_2O)_4Rh(\mu\text{-}OH)_2Cr(OH_2)_4]^{4+}$

A solution prepared by dissolving $[Rh(H_2O)_6][ClO_4]_3\cdot 3H_2O$ (0.5 g) in water (5 cm^3) was placed in an ice–salt water-bath and 1 mol dm^{-3} NaOH (10 cm^3) added with vigorous stirring to give a solution with $[Rh^{III}]$ *ca.* 0.06 mol dm^{-3} and pH > 13. A solution of $[Cr(H_2O)_6][ClO_4]_3$ (30 cm^3, $[Cr] = 0.0294$, $[H^+] \approx 0.17$ mol dm^{-3}) was added dropwise to the above solution over 5–10 min. The final pH was in the range 12–13. The reaction was then quenched by acidification to pH ≈ 1.5 with 1 mol dm^{-3} $HClO_4$, and the resultant homogeneous solution stored at −18 °C until required for purification. Ion-exchange chromatography was used to separate the reaction products. Following adsorption of the reaction mixture onto a Sephadex SP C25 column, elution with acidified 0.5 mol dm^{-3} $NaClO_4$ (40 cm^3) separated the first yellow band from a green band at the top of the column. The band was collected and shown to be $[Rh(H_2O)_6]^{3+}$ from its UV/VIS spectrum.[6] With the addition of 1 mol dm^{-3} $NaClO_4$ (60 cm^3), two green bands began to move down the column, the first being the desired

aqua ion $[(H_2O)_4Rh(\mu\text{-}OH)_2Cr(OH_2)_4]^{4+}$. Successive volumes (30 cm^3) of 2 and 4 mol dm^{-3} $NaClO_4$ were then used to complete elution of the next two fractions and to remove a fourth fraction. A small amount of other green species (presumably aqua ions of higher nuclearity) remained bound to the column. Typical yields were: 21% $[Rh(H_2O)_6]^{3+}$, 55% $[(H_2O)_4Rh(\mu\text{-}OH)_2Cr(OH_2)_4]^{4+}$ and 24% higher polynuclear species.

Equilibrium measurements

The preparation of stock solutions of $[(H_2O)_4Rh(\mu\text{-}OH)_2Cr(OH_2)_4]^{4+}$ with $I \approx 1$ mol dm^{-3} for use in equilibrium measurements involved the absorption of solutions of the cation onto Sephadex SP C25 and elution with either 1.0 mol dm^{-3} $HClO_4$ for studies at high $[H^+]$ or 1.0 mol dm^{-3} $NaClO_4$ (0.02 mol dm^{-3} $HClO_4$) for studies at lower $[H^+]$. The cation concentrations were found to be 0.0115 ± 0.0002 and 0.0122 ± 0.0002 mol dm^{-3}, respectively. The total ionic strength (I) of the two solutions, determined by established methods,[3] was 1.08 mol dm^{-3}.

Equilibrium studies were carried out in the range pH 0–1. Solutions of $[(H_2O)_4Rh(\mu\text{-}OH)_2Cr(OH_2)_4]^{4+}$ were prepared by addition of dimer (d.b.) stock (1.5 cm^3) to standardised $(Na,H)ClO_4$ solutions (3.5 cm^3) such that [d.b.] $\approx 3 \times 10^{-3}$, $[H^+] = 0.1$–1 and $I = 1.0$ mol dm^{-3}. In some solutions $LiClO_4$ was substituted for $NaClO_4$ as a check on specific cation effects. No such effect was observed. These solutions were then equilibrated at various temperatures (288.2–303.2 K), maintained constant (±0.1 K) by placing them in a Haake D8 thermostat connected to a Haake EK12 immersion cooler. The time needed for equilibrium to be reached was estimated from measurements of the rate of interconversion between the s.b. and d.b. forms of the aqua ion. Solutions were left to equilibrate for more than 10 half-lives, then diluted ten-fold with ice-cold 0.1 mol dm^{-3} $HClO_4$ and the previously described, low-temperature (273 K) chromatographic procedure was used to separate the s.b. from the d.b. form.[3] The only change to the procedure was that after elution of a Rh^{3+}–Cr^{3+} mixture (fraction 1) and the d.b. form (fraction 2) with 1 mol dm^{-3} $HClO_4$, the s.b. form (fraction 3) was eluted with 2 mol dm^{-3} $NaClO_4$ rather than 2 mol dm^{-3} $HClO_4$ because the high $[H^+]$ interfered with the rhodium analysis. Rhodium analysis of each fraction enabled determination of $[Rh^{3+}]$, [d.b.] and $[s.b.]_T$. Small amounts of $[Rh(H_2O)_6]^{3+}$ and $[Cr(H_2O)_6]^{3+}$ are present because of some cleavage of the d.b. and s.b. forms during equilibration. Note that $[s.b.]_T$ is the sum of the concentrations of the s.b. form and the monodeprotonated form, s.b. − H, present at equilibrium, *i.e.* $[s.b.]_T = [s.b.] + [s.b. - H]$.

Interconversion kinetics

Solutions of the s.b. form were prepared by dissolving the 'active' hydroxide of the d.b. form in water–concentrated $HClO_4$ (1:1) and allowing the solution to stand at room temperature for 14 h. A pure fraction of the s.b. form was obtained following low-temperature chromatography using 2 mol dm^{-3} $HClO_4$ as eluent. It was stored at −18 °C to minimise cleavage to $[Rh(H_2O)_6]^{3+}$ and $[Cr(H_2O)_6]^{3+}$. It should be stressed, however, that small amounts of the monomeric complexes do not interfere with the study of the s.b.–d.b. interconversion since their concentration will remain constant throughout the reaction. Prior to use in the kinetic studies, solutions of the s.b. form were diluted 1:1 with distilled water to give a final $[H^+]$ of approximately 1 mol dm^{-3}. The exact $[H^+]$ and [s.b.] were determined as indicated above. Three stock solutions of s.b. with known $[H^+]$ (0.97–1.07 mol dm^{-3}) and [s.b.] (0.0183–0.0311 mol dm^{-3}) were used in this study. The UV/VIS spectrum of s.b. was recorded in 1 mol dm^{-3} $HClO_4$ and is compared to that of d.b. in Fig. 1.

For kinetic runs at pH < 1.2 reaction mixtures were prepared by adding the stock solution of the s.b. form (0.2 cm^3) to $(Na,H)ClO_4$ mixtures (2.8 cm^3) which were kept at thermal equilibrium in a spectrophotometer cell, while for runs at pH > 1.2 the same stock solution (0.2 cm^3) was added to solutions (2.8 cm^3) containing appropriate amounts of NaOH and $NaClO_4$. This gave [s.b.] = (1.22–2.07) × 10^{-3} and $I = 1.0$ mol dm^{-3}. Variable-wavelength kinetic runs showed that significant changes in absorbance occurred as the reaction proceeded and that the rate constant did not vary with λ. The reaction was monitored at 250 nm where increases in absorbance of 0.1–0.4 were observed. At the highest pH values slight increases in absorbance were found well after the interconversion reaction was complete, indicating that some polymerisation is taking place. Although this made the determination of A_∞ difficult it had no measurable effect on the absorbance data over the initial five half-lives of the interconversion reaction. Consequently, the data were fitted using the equation $A_t = A_\infty - (A_0 - A_\infty)e^{-k_{obs}t}$ and A_0, A_∞ and k_{obs} were all determined as part of the analysis.

Cleavage kinetics

A stock solution of $[(H_2O)_4Rh(\mu\text{-}OH)_2Cr(OH_2)_4]^{4+}$ with [d.b.] = 0.0190 ± 0.0003, $[H^+] = 0.020 \pm 0.003$ and $I \approx 1$ mol dm^{-3} was prepared by eluting the aqua ion with 1.0 mol dm^{-3} $NaClO_4$ (0.02 mol dm^{-3} $HClO_4$). This solution was used in all of the kinetic experiments. Typical reaction mixtures were prepared at the desired temperature (343–363 K) by mixing the stock solution (0.5 cm^3) with a series of solutions containing various proportions of $HClO_4$ and $NaClO_4$ (2.5 cm^3). The final reaction conditions were [d.b.] = 3.17 × 10^{-3}, $[HClO_4]$ = 0.083–0.862 and $I = 1.0$ mol dm^{-3} ($NaClO_4$). In the analysis of the kinetic data these acid concentrations were corrected for the temperature-dependent expansion of the solvent. The reaction was monitored at 275 nm where absorbance decreases of 0.3–0.5 units were observed. Rate constants, k_{obs}, were determined by least-squares fitting of the change in absorbance with time to the expression $A_t = (A_0 - A_\infty)e^{-k_{obs}t} + A_\infty$. In most cases, A_0, A_∞ and k_{obs} were all determined as part of the data analysis. In some cases the experimentally determined A_∞ values were used in the calculation of k_{obs}. The values of k_{obs} obtained from the two treatments were in excellent agreement as were the experimental and fitted A_∞ values. The values of k_{obs} did not vary with λ.

Results

Equilibrium measurements

Initial experiments revealed that when solutions of $[(H_2O)_4Rh(\mu\text{-}OH)_2Cr(OH_2)_4]^{4+}$ were allowed to stand in acidic solution ($[H^+] \approx 1$ mol dm^{-3}, both $[(H_2O)_5Rh(\mu\text{-}OH)Cr(OH_2)_5]^{5+}$ (s.b. form) and $[(H_2O)_4Rh(\mu\text{-}OH)_2Cr(OH_2)_4]^{4+}$ (d.b. form) could be isolated using ion-exchange chromatography. The UV/VIS spectrum of the former differs significantly from that of the latter (Fig. 1). The overall charge and similarity in solution behaviour to that of the chromium(III) singly bridged dimer indicate the formation of a singly bridged heterometallic aqua ion. Despite the difference in spectra, attempts to measure the equilibrium constant for the s.b.–d.b. rearrangement reaction using this technique were unsuccessful because the spectral changes were generally small and irreproducible. Instead, solutions of d.b. in varying concentrations of H^+ were left to equilibrate at various temperatures (288.2–303.2 K) and ion-exchange chromatography at 273 K used to separate the s.b. from the d.b. species. Under these conditions the rate of interconversion is extremely slow, and slower than in the case of the chromium(III) dimer (see below) where it was previously shown that dilution with acid and changes in temperature do not cause changes in the

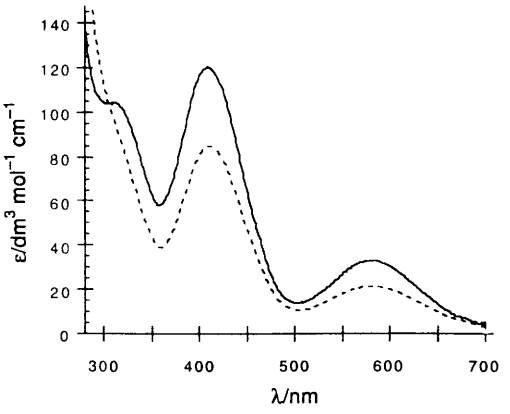

Fig. 1 The UV/VIS spectrum of $[(H_2O)_4Rh(\mu\text{-}OH)_2Cr(OH_2)_4]^{4+}$ recorded in 1 mol dm^{-3} $NaClO_4$–0.01 mol dm^{-3} $HClO_4$ (– – –) and of $[(H_2O)_5Rh(\mu\text{-}OH)Cr(OH_2)_5]^{5+}$ in 1 mol dm^{-3} $HClO_4$ media (——)

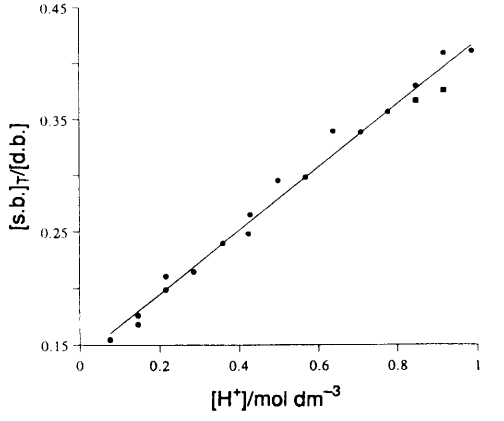

Fig. 2 Dependence of $[s.b.]_T/[d.b.]$ on acid concentration at 298.2 K and I = 1.0 mol dm^{-3} (●, $NaClO_4$; ■, $LiClO_4$ medium)

equilibrium concentrations of the s.b. and d.b. species.[3] Three separate fractions were obtained: the first containing a mixture of Rh^{3+} and Cr^{3+}, the second the d.b. form and the third the total (T) of all singly bridged species at equilibrium. As in the case of chromium(III) dimer, the s.b. species present at equilibrium absorbed onto the column as the fully protonated form (charge + 5) and were eluted as one fraction.

The linear dependence of $[s.b.]_T/[d.b.]$ on $[H^+]$ (Fig. 2) is interpreted in terms of the equilibria shown in Scheme 1 which is related to that used to describe the chromium(III) dimer equilibrium.[3] The acid dependence arises from deprotonation of the s.b. form, the high charge of which coupled with hydrogen-bond stabilisation on deprotonation gives rise to a high acidity. Two parameters describe the s.b.–d.b. equilibrium: K_{a1} the first acid-dissociation constant of the s.b. form and K_1 the constant for the equilibrium between s.b. – H and the d.b. form, see equation (1). Linear least-squares analysis of the data

$$\frac{[S.B.]_T}{[D.B.]} = \frac{[H^+]}{K_1K_{a1}} + \frac{1}{K_1} \quad (1)$$

gave $1/K_1$ and $1/K_1K_{a1}$ from which the K_1, K_{a1} and K_1K_{a1} ($=K_{eq}$) values listed in Table 1 and the thermodynamic parameters listed in Table 2 were determined.

Interconversion kinetics

The rates of interconversion between the s.b. and d.b. forms have been determined in the ranges pH 0–2.8 and 288.2–303.2 K from absorbance changes observed at 250 nm. The reaction could not be followed at higher pH because of the lack of suitable non-co-ordinating buffers with pK_a values in the region of 3–5 which do not absorb in the UV region, and the changes in the visible spectrum were too small to enable the reaction to be followed in this region. A first-order reaction in [s.b.] was indicated by the excellent fits to the absorbance data obtained over the whole pH range used. Full listings of k_{obs} values are available as supplementary material (SUP 57117).

The pH dependence of k_{obs} at 298.2 K (Fig. 3) shows two regions where small increases in rate are observed, 0.2–1 and

Table 1 Temperature dependence of equilibrium constants for the s.b.–d.b. interconversion of $[(H_2O)_4Rh(\mu\text{-}OH)_2Cr(OH_2)_4]^{4+}$

T/K	K_1	$K_{eq} = K_1K_{a1}$/mol dm^{-3}	K_{a1}/mol dm^{-3}
288.2	8.56(0.56)	2.252(0.065)	0.263(0.025)
293.2	8.38(0.57)	2.578(0.093)	0.308(0.032)
298.2	7.20(0.26)	3.56(0.10)	0.495(0.032)
303.2	6.67(0.30)	4.18(0.18)	0.627(0.055)

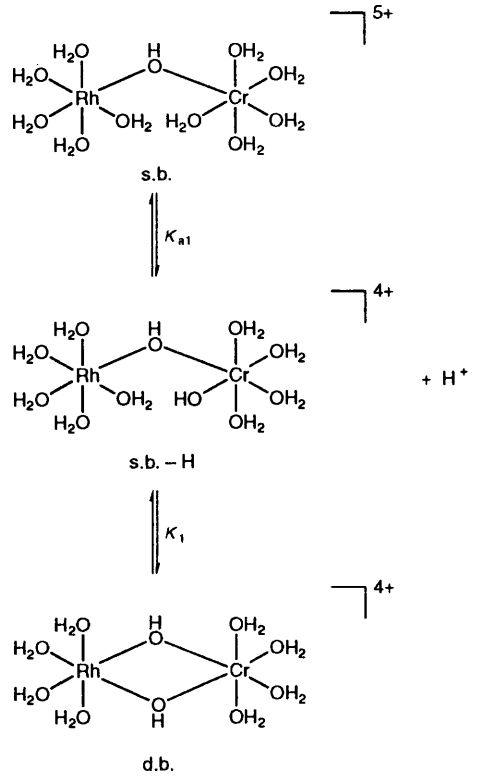

Scheme 1

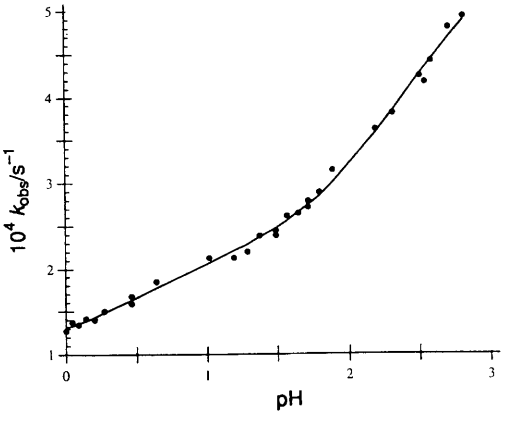

Fig. 3 pH Dependence of the observed rate constant (k_{obs}, ●) for the s.b.–d.b. interconversion of $[(H_2O)_4Rh(\mu\text{-}OH)_2Cr(OH_2)_4]^{4+}$ at 298.2 K. Curve based on equation (4)

Table 2 Equilibrium constants and thermodynamic parameters for the interconversion of $[A_4(H_2O)M(\mu\text{-}OH)M'(OH_2)A_4]^{5+}$ and $[A_4M(\mu\text{-}OH)_2M'A_4]^{4+}$

System	Parameter[a]	Value at 298 K	$\Delta H°$/ kJ mol^{-1}	$\Delta S°$/ J K^{-1} mol^{-1}
M = Rh, M′ = Cr, $A_4 = (H_2O)_4$	K_{a1}	0.5	45(6)	146(22)
	K_1	7.1	−13(2)	−28(8)
	K_{eq}	3.3	32(4)	117(14)
M = M′ = Cr, $A_4 = (H_2O)_4$[b]	K_{a1}	0.18	43(4)	128(13)
	K_1	10.1	−10(3)	−15(9)
	K_{eq}	1.83	30(1)	104(4)
M = M′ = Ir, $A_4 = (H_2O)_4$[c]	K_{a1}	0.16		
M = M′ = Cr, $A_4 = (NH_3)_4$[d]	K_{a1}	0.014	49(6)	129(20)
	K_1	3.1	−6(4)	−11(14)
	K_{eq}	0.042	43(10)	118(34)
M = M′ = Cr, $A_4 = (en)_2$[d]	K_{a1}	0.29	12(3)	30(9)
	K_1	1.33	3.1(9)	13(3)
	K_{eq}	0.40	15(4)	43(12)
M = M′ = Rh, $A_4 = (NH_3)_4$[d]	K_{a1}	3.9×10^{-4}	53(2)	111(5)
	K_1	0.33	−2(1)	−15(4)
	K_{eq}	1.3×10^{-4}	51(3)	96(9)
M = M′ = Rh, $A_4 = (en)_2$[d]	K_{a1}	4.3×10^{-3}	28(4)	49(13)
	K_1	0.089	14(3)	28(8)
	K_{eq}	3.8×10^{-4}	42(7)	77(21)
M = M′ = Ir, $A_4 = (en)_2$[d]	K_{a1}	0.012	11(7)	−1(22)
	K_1	0.18	2(5)	−10(15)
	K_{eq}	2.2×10^{-3}	13(12)	−11(37)

[a] Units for K_{a1} and K_{eq} ($= K_1K_{a1}$) are mol dm^{-3}. [b] Data from ref. 3. [c] Data from ref. 10. [d] Data from refs. 9 and 11.

1.5–3. The data are interpreted in terms of three pathways which are shown in Scheme 2. These involve the fully protonated (s.b.), monodeprotonated (s.b. − H) and doubly deprotonated (s.b. − 2H) singly bridged complexes. This interpretation is consistent with previous work on the chromium(III) dimer,[4] and with measurements of the equilibrium between the s.b. and d.b. forms at low pH. The equilibrium measurements show that significant amounts of s.b., s.b. − H and d.b. are present at equilibrium. This information supports the conclusion that for the s.b. and s.b. − H pathways both the forward and back reactions contribute to k_{obs}. At high pH ($\geqslant 2$) the small increase in rate is attributed to the s.b. − 2H pathway which is expected to lead to the d.b. form at a faster rate than either the s.b. or s.b. − H path.

The rate law for the s.b.–d.b. interconversion is given by equation (2) from which the expression (3) for k_{obs} can be

$$d[d.b.]_T/dt = k_0[s.b.] + k_1[s.b. - H] + k_2[s.b. - 2H] - k_{-0}[d.b. + H] - k_{-1}[d.b.] - k_{-2}[d.b. - H] \quad (2)$$

$$k_{obs} = \left[\frac{k_0[H^+]^2 + k_1K_{a1}[H^+] + k_2K_{a1}K_{a2}}{[H^+]^2 + K_{a1}[H^+] + K_{a1}K_{a2}}\right] + \left\{\frac{k_{-0}K_{p3}[H^+] + k_{-1} + (k_{-2}/K_{p4}[H^+])}{K_{p3}[H^+] + 1 + (1/K_{p4}[H^+])}\right\} \quad (3)$$

derived following application of the appropriate acid–base equilibria. This expression can be significantly simplified because K_{p3} is expected to be small for a 4+ ion ($\ll 0.1$ dm^3 mol^{-1}), as is the case for the chromium(III) dimer.[7] In addition, chromatographic analyses showed that the amount of s.b. species present at completion of the reaction was below the limit of detection (*ca.* 2–3%) for runs carried out at or above pH $\approx$ 2.3. This means that at this and higher pH the contribution of the three back reactions to k_{obs}, either individually or in total, is small and thus the contribution of the k_{-2} pathway is small under these conditions. Modification of equation (3) to incorporate these findings and substitution of $k_{-0}K_{p3}$ and k_{-1} by k_0/K_{eq} and k_1K_{a1}/K_{eq}, respectively, gives expression (4). Previously determined values of K_{a1} and K_{eq} were used in the fitting of the data by equation (4). Although large increases in rate were not observed at high pH, attempts to fit the data

$$k_{obs} = \left(\frac{k_0[H^+]^2 + k_1K_{a1}[H^+] + k_2K_{a1}K_{a2}}{[H^+]^2 + K_{a1}[H^+] + K_{a1}K_{a2}}\right) + \left(\frac{k_0[H^+] + k_1K_{a1}}{K_{eq}}\right) \quad (4)$$

without allowances for k_2 and K_{a2} led to systematic variations between fitted and observed values and very large uncertainties in each parameter. The data were fitted using a least-squares procedure with good fits obtained at all temperatures (Fig. 3 shows the fit at 298.2 K). This further supports the model chosen to describe the s.b. and d.b. interconversion. The parameters are listed in Table 3 along with the values of $k_{-0}K_{p3}$ and k_{-1}, calculated using $k_{-0}K_{p3} = k_0/K_{eq}$ and $k_{-1} = k_1/K_1 = k_1K_{a1}/K_{eq}$, respectively. Activation parameters and thermodynamic constants are listed in Table 4.

Cleavage kinetics

The rate of cleavage of $[(H_2O)_4Rh(\mu\text{-}OH)_2Cr(OH_2)_4]^{4+}$ (d.b. form) to $[Rh(H_2O)_6]^{3+}$ and $[Cr(H_2O)_6]^{3+}$ has been determined at various $[H^+]$ and temperatures, by fitting the change in absorbance by a first-order expression (SUP 57117). Chromatographic analysis showed that only $[Rh(H_2O)_6]^{3+}$ and $[Cr(H_2O)_6]^{3+}$ were present at the end of the reaction and that the reaction is irreversible under the conditions employed. Although these ions have the same charge and predominantly elute together, small amounts of $[Cr(H_2O)_6]^{3+}$ were eluted first, followed by a mixture of the two and finally a small amount of $[Rh(H_2O)_6]^{3+}$. The UV/VIS spectrum confirmed the presence of $[Cr(H_2O)_6]^{3+}$ and $[Rh(H_2O)_6]^{3+}$.

The dependence of k_{obs} on $[H^+]$ (Fig. 4) is effectively linear with a non-zero intercept and indicates that at least two pathways contribute to the reaction rate, one of which is acid dependent. However, the dependence should be slightly curved because a pre-equilibrium is established between the s.b. and d.b. forms, for which thermodynamic constants have been determined (see above).

The reaction pathways responsible for the cleavage of $[(H_2O)_4Rh(\mu\text{-}OH)_2Cr(OH_2)_4]^{4+}$ are shown in Scheme 3. The

Table 3 Rate and acid-dissociation constants for the s.b.–d.b. interconversion of $[(H_2O)_4Rh(\mu\text{-}OH)_2Cr(OH_2)_4]^{4+}$

T/K	10^5k_0/s^{-1}	10^5k_1/s^{-1}	10^5k_2/s^{-1}	10^2K_{a2}/mol dm^{-3}	10^5k_{-1} [a]/s^{-1}	$10^5k_{-0}K_{p3}$ [b]/dm^3 mol^{-1}
288.2	1.01(0.06)	5.05(0.09)	13.8(1.9)	0.240(0.081)	0.59(0.08)	0.45(0.04)
293.2	2.14(0.20)	10.19(0.23)	23.4(3.0)	0.26(0.10)	1.22(0.20)	0.83(0.11)
298.2	4.29(0.48)	19.11(0.43)	57.0(1.8)	0.381(0.051)	2.65(0.31)	1.20(0.17)
303.2	5.8(1.2)	38.3(1.0)	82.6(5.6)	0.60(0.18)	5.74(0.91)	1.38(0.36)

[a] Calculated from $k_{-1} = k_1/K_1$, using k_1 and K_1 from Table 1. [b] Calculated from $k_{-0}K_{p3} = k_0/K_{eq}$, using k_0 and K_{eq} from Table 1.

Table 4 Activation parameters and thermodynamic constants for the s.b.–d.b. interconversion of $[(H_2O)_4Rh(\mu\text{-}OH)_2Cr(OH_2)_4]^{4+}$ and $[(H_2O)_4Cr(\mu\text{-}OH)_2Cr(OH_2)_4]^{4+}$

	$[(H_2O)_4Rh(\mu\text{-}OH)_2Cr(OH_2)_4]^{4+}$			$[(H_2O)_4Cr(\mu\text{-}OH)_2Cr(OH_2)_4]^{4+}$ [a]		
Parameter [b]	Value at 298 K [c]	$\Delta H^{\ddagger\circ}$/kJ mol^{-1}	$\Delta S^{\ddagger\circ}$/J K^{-1} mol^{-1}	Value at 298 K	$\Delta H^{\ddagger\circ}$/kJ mol^{-1}	$\Delta S^{\ddagger\circ}$/J K^{-1} mol^{-1}
$10^5\,k_0$	3.9	92(8)	−21(26)	10.1	88(3)	−26(11)
$10^5\,k_1$	20	95(2)	1(5)	41.7	92(1)	0(2)
$10^5\,k_2$	53	88(15)	−13(50)	1140	67(2)	−58(6)
K_{a1}	0.5 [d]	45(6) [d]	146(22) [d]	0.101	48(4)	141(12)
$10^2\,K_{a2}$	0.39	44(11)	100(36)	0.0054	68(3)	147(10)
$10^5\,k_{-1}$	2.7	107(2)	28(8)	2.2	110(5)	35(16)
$10^5\,k_{-0}K_{p3}$	1.1	60(9)	−80(30)	5.2	59(2)	−130(8)
K_1	7.1 [d]	−13(2) [d]	−28(7) [d]	19	−19.6(5)	−41(17)

[a] Data from kinetic studies (ref. 4); K_{a1} and K_1 differ slightly from those in ref. 3. [b] Units: s^{-1} for k_0, k_1, k_2, k_{-1}; dm^3 mol^{-1} s^{-1} for $k_{-0}K_{p3}$; mol dm^{-3} for K_{a1} and K_{a2}. [c] As calculated from thermodynamic and activation parameters. [d] Data taken from Table 2.

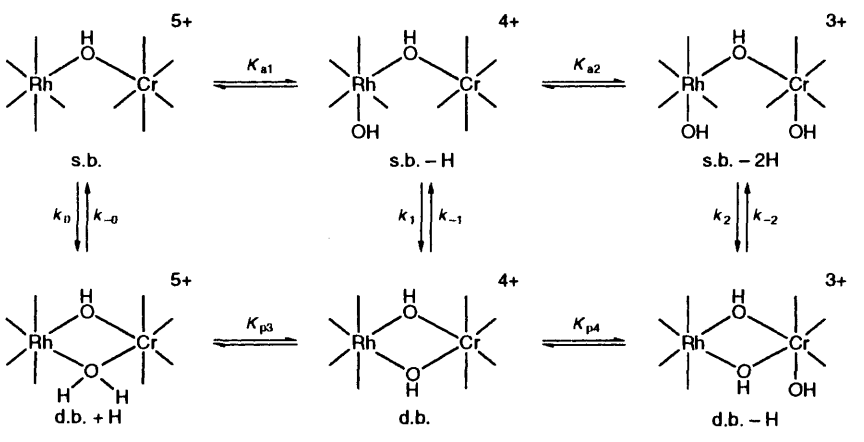

Scheme 2

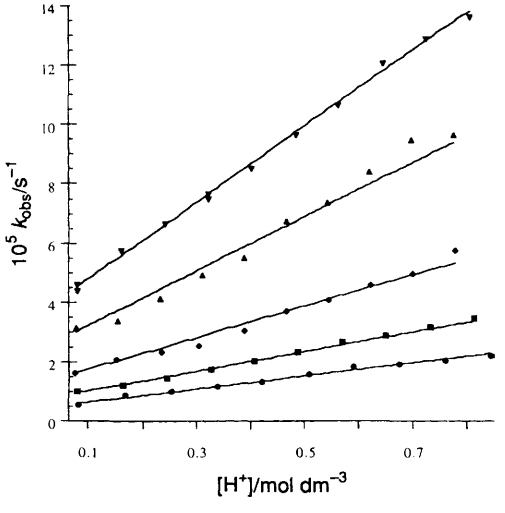

Fig. 4 Acid concentration and temperature dependences of k_{obs} for cleavage of $[(H_2O)_4Rh(\mu\text{-}OH)_2Cr(OH_2)_4]^{4+}$. Full lines represent values determined from equation (7) (●, 343.4; ■, 348.3; ◆, 353; ▲, 359.2; ▼, 363.2 K)

overall process involves several pathways which can be divided into two categories, equilibration between the d.b. and s.b. forms, which is then followed by rate-determining cleavage of the s.b. forms to give $[Rh(H_2O)_6]^{3+}$ and $[Cr(H_2O)_6]^{3+}$. Interconversion between the s.b. and d.b. forms is > 100 times faster than cleavage of the s.b. forms. Thus, the rate constants of importance are $k_{s.b.}$ and $k_{s.b.-H}$, which represent cleavage of s.b. and s.b. − H, respectively. Scheme 3 indicates that the acid dependence of k_{obs} arises from the protonation equilibrium between forms s.b. and s.b. − H and that the cleavage processes are acid independent. Since only $[Rh(H_2O)_6]^{3+}$ and $[Cr(H_2O)_6]^{3+}$ are present at the end of the reaction and hence the reaction is irreversible, k_{10} and k_{11} must be small.

From the rate law (5) for cleavage of the d.b. form, equation (6) can be derived, where $k_{uc} = k_{s.b.-H}/K_1$ and $k_c = k_{s.b.}/K_{eq}$.

$$d[M^{3+}]/dt = k_{s.b.}[\text{s.b.} - \text{H}] + k_{s.b.}[\text{s.b.}] \quad (5)$$

$$\frac{d[M^{3+}]}{dt} = \left\{\frac{k_{uc} + k_c[H^+]}{1 + (1/K_1) + ([H^+]/K_{eq})}\right\}[\text{d.b.}]_T = k_{obs}[\text{d.b.}]_T \quad (6)$$

Taking into account the temperature dependence of each parameter, expression (7) can be written for k_{obs}. In analysing

Table 5 Kinetic and thermodynamic data for acid cleavage of $[(H_2O)_4Rh(\mu\text{-}OH)_2Cr(OH_2)_4]^{4+}$ and $[(H_2O)_4Cr(\mu\text{-}OH)_2Cr(OH_2)_4]^{4+}$

	$[(H_2O)_4Rh(\mu\text{-}OH)_2Cr(OH_2)_4]^{4+}$			$[(H_2O)_4Cr(\mu\text{-}OH)_2Cr(OH_2)_4]^{4+}$ [b]		
Parameter [a]	Value at 298 K	$\Delta H^{\ddagger}/^{\circ}$/ kJ mol^{-1}	$\Delta S^{\ddagger}/^{\circ}$/ J K^{-1} mol^{-1}	Value at 298 K	$\Delta H^{\ddagger}/^{\circ}$/ kJ mol^{-1}	$\Delta S^{\ddagger}/^{\circ}$/ J K^{-1} mol^{-1}
$10^7 k_{uc}$/s^{-1}	0.10	112(4)	38(13)	0.38	109(1)	35(2)
$10^7 k_c$/dm^3 mol^{-1} s^{-1}	1.7	95(3)	0(9)	14.6	83(1)	−22(2)
$10^7 k_{s.b.-H}$/s^{-1}	0.74	99(7)	10(21)	3.9	98(3)	20(11)
$10^7 k_{s.b.}$/s^{-1}	5.9	126(7)	117(23)	27(2)	112(2)	83(5)
$10^7 k_{-1}$ [b]/s^{-1}	270	107(2)	28(8)	220(10)	110(5)	35(16)
$10^7 k_{-0}K_{p3}$/dm^3 mol^{-1} s^{-1}	110	60(9)	−80(30)	520(10)	59(2)	−130(8)
$10^7 k_{-0}$/s^{-1}	1100 [c]	105 [d]	66 [d]	5200 [e]	104 [e]	0 [e]

[a] Data taken from ref. 5. [b] Data from Table 4. [c] Estimated from $k_{-0}K_{p3}$ assuming $K_{p3} \approx 0.1$ dm^3 mol^{-1}. [d] Activation parameters for k_{-0} estimated from parameters for $k_{-0}K_{p3}$ and assuming $\Delta H^{\circ}(K_{p3}) \approx -45$ kJ mol^{-1} and $\Delta S^{\circ}(K_{p3}) \approx -130$ J K^{-1} mol^{-1}. [e] Estimated.

$$K_{obs} = \frac{\frac{kT}{h}\left\{\exp\left[\frac{\Delta H^{*}(k_{uc}) - T\Delta S^{*}(k_{uc})}{RT}\right] + [H^+]\exp\left[\frac{\Delta H^{*}(k_c) - T\Delta S^{*}(k_c)}{RT}\right]\right\}}{1 + \left\{\exp\left[\frac{-\Delta H^{\circ}(K_1) + T\Delta S^{\circ}(K_1)}{RT}\right] + [H^+]\exp\left[\frac{-\Delta H^{\circ}(K_{eq}) + T\Delta S^{\circ}(K_{eq})}{RT}\right]\right\}} \quad (7)$$

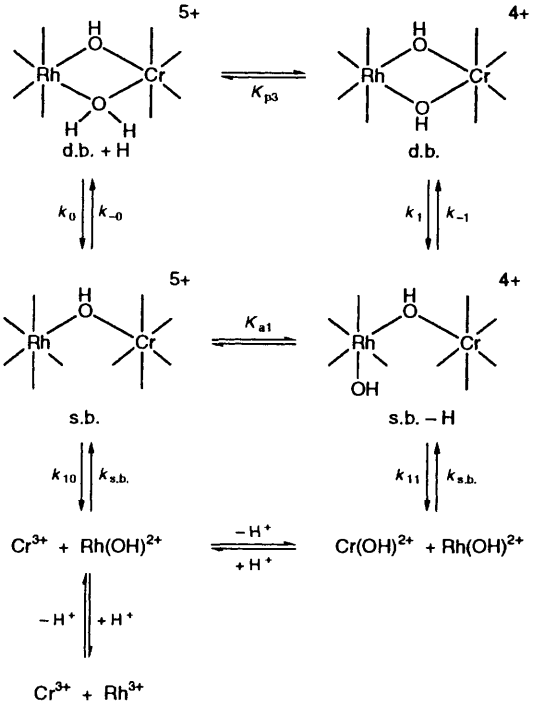

Scheme 3

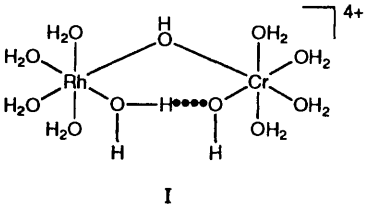

I

the data, values of K_1 and K_{eq} derived from equilibrium studies (Table 2) were used to reduce the number of parameters in equation (7). Weighted non-linear least-squares analysis of the temperature and $[H^+]$ dependence of k_{obs} gave the activation parameters listed in Table 5 from which k_{uc} and k_c were calculated at 298 K. The data were weighted against $[1/\sigma(k_i)]^2$. From these values and those of K_1 and K_{eq} (Table 1), $k_{s.b.-H}$, $k_{s.b.}$ and their respective activation parameters have been estimated using $k_{s.b.-H} = K_1 k_{uc}$ and $k_{s.b.} = k_c K_{eq}$ and are also listed in Table 5.

Discussion

In strongly acidic solution the heteropolynuclear aqua ion $[(H_2O)_4Rh(\mu\text{-}OH)_2Cr(OH_2)_4]^{4+}$ d.b. form is converted into a singly bridged (s.b.) form $[(H_2O)_5Rh(\mu\text{-}OH)Cr(OH_2)_5]^{5+}$ with different solution properties. The equilibrium between the two forms involves two processes (Scheme 1), deprotonation/protonation of s.b. (K_{a1}) and intramolecular interconversion between the monodeprotonated s.b. and d.b. forms (K_1), as has been established for the rearrangement of the chromium(III) dimer [3] and several monools $[A_4(H_2O)M(\mu\text{-}OH)M(OH_2)A_4]^{5+}$ [M = Cr, Rh or Ir; $A_4 = (NH_3)_4$ or $(en)_2$ (en = ethane-1,2-diamine)] to the diols $[A_4M(\mu\text{-}OH)_2MA_4]^{4+}$.[9] The significantly higher acidity of $[(H_2O)_5Rh(\mu\text{-}OH)Cr(OH_2)_5]^{5+}$ ($K_{a1} = 0.5$ mol dm^{-3}) compared with the s.b. dimers of Cr^{III} ($K_{a1} = 0.18$)[3] and the Ir^{III} ($K_{a1} = 0.16$ mol dm^{-3})[10] reflects either a greater degree of hydrogen-bond stabilisation for the monodeprotonated heterometallic aqua ion or a greater acidity of the rhodium(III) centre. The greater acidity of rhodium(III) aqua ions compared with analogous chromium(III) ions is well established [6,12–14] as is the enhancement in acidity achieved through hydrogen-bond stabilisation of the monodeprotonated aqua ions (Structure I).[3,9,10] Much higher K_{a1} values have been found for complexes of similar charge but where the monodeprotonated forms are not stabilised through hydrogen-bonding, *e.g.* $[(H_3N)_5Cr(\mu\text{-}OH)Cr(NH_3)_4(OH_2)]^{5+}$.[9] The higher acidity of $[(H_2O)_5Rh(\mu\text{-}OH)Cr(OH_2)_5]^{5+}$ has little effect on the thermodynamic parameters which are similar to those for s.b. chromium(III) dimers and the NH_3 monools, but are higher than for the en monool (Table 2).[9]

The equilibrium constant for the rearrangement of the s.b. − H to d.b. form, $K_1 = 7.1$, is comparable to that reported for the chromium(III) dimer ($K_1 = 10.1$).[3] Hydrogen-bond stabilisation of the monodeprotonated s.b. form reduces the magnitude of K_1, so that the actual equilibrium constant for its rearrangement to the d.b. form is actually larger than K_1. Comparison of these values with those for related homometallic monools (Table 2) reveals that K_1 is larger for the chromium(III) than for the rhodium(III) systems indicating that the d.b. forms are more stable for the former. The similarity in the values of K_1 for the Cr^{III}–Rh^{III} aqua ion and the chromium(III) dimer is

consistent with a Cr^{III}-centred process for the heterometallic ion (see later). Stabilisation of the s.b. − H over the d.b. form with temperature is indicated by the thermodynamic constants associated with K_1 and overrides the expected decrease in hydrogen-bond stabilisation with temperature. Thus, the increase in [d.b.] with temperature arises primarily from an increase in [s.b. − H] attributable to a rise in the acidity of the s.b. form.

The kinetics of interconversion between the s.b. and d.b. forms of $[(H_2O)_4Rh(\mu\text{-}OH)_2Cr(OH_2)_4]^{4+}$ have been interpreted in terms of the pathways in Scheme 2 in which ring closure within the s.b., s.b. − H (monodeprotonated) and s.b. − 2H (doubly deprotonated) forms, and ring opening within the d.b. and d.b. − H (monodeprotonated) forms contribute to the rate. Thus, the interconversion between the s.b. and d.b. forms of the heterometallic ion occurs through the same reaction pathways as for the chromium(III) dimer[4] and, at low pH, it also parallels the ring-closure reactions of the monools $[A_4(H_2O)M(\mu\text{-}OH)M(OH_2)A_4]^{5+}$ [M = Cr, Rh or Ir; A_4 = $(NH_3)_4$ or $(en)_2$].[9] The correspondence of the reaction rates (see Table 4) to those for the chromium(III) dimer indicates that the reactions are Cr^{III}-centred. This view is strongly supported by recent oxygen-18 labelling and oxygen-17 NMR measurements of the rate of water exchange on a rhodium(III) dimer.[4] These have clearly shown that water ligands *trans* to the bridging OH groups exchange at a faster rate than *cis* water ligands and, moreover, that both rate constants were over 100 times slower than for the corresponding process on a chromium(III) dimer. In addition, unlike in the case of the chromium(III) dimer, exchange of the bridging OH groups on the rhodium(III) dimer could not be detected during the course of the water-exchange reaction indicating that bridge-opening processes are much slower for the latter dimer. The activation and thermodynamic parameters for the chromium(III) dimer[4] and $[(H_2O)_4Rh(\mu\text{-}OH)_2Cr(OH_2)_4]^{4+}$ (Table 4) provide strong support for this proposal. The values of $\Delta H^{\ddagger}$ and $\Delta S^{\ddagger}$ for k_0, k_1, k_{-1} and $K_{p3}k_{-0}$ for the two systems are the same within experimental uncertainties as are the values of ΔH° and ΔS° associated with K_{a1} and K_1. The arguments in favour of a reaction mechanism which is more associative than dissociative previously elaborated for the chromium(III) system also apply here.[4]

Double deprotonation results in a small increase in overall rate ($k_2 \approx 2.5k_1$) compared with chromium(III) dimer where the increase was *ca.* 25 fold. Given the similarities of the rate profiles for the two systems, a larger rate increase might have been anticipated. The second deprotonation is probably occurring at a water molecule co-ordinated to the Rh^{III}. Thus, if reaction involves substitution at Cr^{III} then double deprotonation will have little effect on the ring-closure reaction. Under these circumstances the activation parameters for k_2 would be similar to those for the other ring-closure pathways. Although this is the case, the data need to be interpreted cautiously because of the large errors in $\Delta H^{\ddagger}$ and $\Delta S^{\ddagger}$. There is also the possibility that deprotonation at Rh^{III} may labilise this centre sufficiently to allow the reaction to occur *via* substitution at this centre. An increase in lability of 100 fold would be sufficient to bridge the difference in the rates of substitution at Cr^{III} and Rh^{III}.[14-17] While rate enhancements of this magnitude have been observed for the intramolecular rearrangement of a rhodium(III) trimer,[18] the effects were only of the order of 3–6 fold for water exchange on a rhodium(III) dimer.[14]

Cleavage of $[(H_2O)_4Rh(\mu\text{-}OH)_2Cr(OH_2)_4]^{4+}$ to the parent aqua ions involves two pathways, cleavage of the s.b. and s.b. − H forms, and the acid dependence is attributed to the establishment of the s.b.–d.b. equilibrium. The rate constants for the two cleavage paths are only about 5 times slower than those for the chromium(III) dimer and the activation parameters for the two systems are within the experimental uncertainties (Table 5).[5] Preliminary investigations indicate that cleavage of the rhodium(III) dimer is substantially slower under the same reaction conditions.[18] Thus, the cleavage of $[(H_2O)_4Rh(\mu\text{-}OH)_2Cr(OH_2)_4]^{4+}$ is also thought to involve substitution at Cr^{III} rather than Rh^{III}. The subtle variations in rate constants for the two systems, which are observed for most of the interconversion processes described earlier and the two cleavage processes, are attributed to small electronic effects accompanying the replacement of one Cr^{III} centre by Rh^{III} and possibly to changes in the degree of hydrogen-bond stabilisation of the monodeprotonated s.b. form.

Cleavage of the d.b. forms of the Rh^{III}–Cr^{III} aqua ion is faster than that of the s.b. form as both k_{-1} (270×10^{-7} s^{-1}) and k_{-0} (estimated 1100×10^{-7} s^{-1}) are substantially larger than $k_{s.b.-H}$ (0.74×10^{-7} s^{-1}) and $k_{s.b.}$ (5.9×10^{-7} s^{-1}). Thus, the extra bridging group in the d.b. forms significantly enhances the cleavage rates. A correlation between the OH/Cr ratio and the rate of hydrolytic processes has previously been elaborated for the chromium(III) oligomers.[17] This is expected to hold for the heterometallic aqua ion studied here because substitution also occurs at the chromium(III) centre.

Acknowledgements

We are grateful to the Australian Research Council for financial support. S. J. C. acknowledges financial assistance in the form of an Australian Postgraduate Award.

References

1 S. J. Crimp, G. D. Fallon and L. Spiccia, *J. Chem. Soc., Chem. Commun.*, 1992, 197.
2 M. R. Grace and L. Spiccia, *Polyhedron*, 1991, **10**, 2389.
3 T. Merakis and L. Spiccia, *Aust. J. Chem.*, 1989, **42**, 1579.
4 L. Spiccia and W. Marty, *Polyhedron*, 1991, **10**, 619.
5 L. Spiccia, *Polyhedron*, 1991, **10**, 1865.
6 R. Cervini, G. D. Fallon and L. Spiccia, *Inorg. Chem.*, 1991, **30**, 831.
7 G. H. Ayres, B. L. Tuffly and J. S. Forrester, *Anal. Chem.*, 1955, **27**, 1742.
8 G. H. Ayres and F. Young, *Anal. Chem.*, 1952, **24**, 155.
9 J. Springborg, *Adv. Inorg. Chem.*, 1988, **32**, 55.
10 S. E. Castillo-Blum, D. T. Richens and A. G. Sykes, *Inorg. Chem.*, 1989, **28**, 954.
11 F. Christensson and J. Springborg, *Acta Chem. Scand., Sect. A*, 1982, **36**, 21.
12 H. Stunzi and W. Marty, *Inorg. Chem.*, 1983, **22**, 2145.
13 G. H. Ayres and S. J. Forrester, *J. Phys. Chem.*, 1959, **63**, 1979; W. Plumb and G. M. Harris, *Inorg. Chem.*, 1964, **3**, 542.
14 A. Drljaca, L. Spiccia, H. R. Krouse and T. W. Swaddle, *Inorg. Chem.*, in the press.
15 F.-C. Xu, H. R. Krouse and T. W. Swaddle, *Inorg. Chem.*, 1985, **24**, 267.
16 G. Laurenczy, I. Rapaport, D. Zbinden and A. E. Merbach, *Magn. Reson. Chem.*, 1991, **29**, S45.
17 S. J. Crimp, L. Spiccia, H. R. Krouse and T. W. Swaddle, *Inorg. Chem.*, 1994, **33**, 465.
18 S. J. Crimp and L. Spiccia, Ph.D. Thesis, Monash University, 1994.

Received 8*th August* 1995; *Paper* 5/05312I